PHYSICAL REVIEW B VOLUME 45, NUMBER 16 15 APRIL 1992-II

Electroluminescence investigations of electron and hole resonant tunneling in *p-i-n* double-barrier structures

C. R. H. White, H. B. Evans, L. Eaves, P. M. Martin, and M. Henini
Department of Physics, University of Nottingham, Nottingham, NG7 2RD, United Kingdom

G. Hill and M. A. Pate
Department of Electronic Engineering, University of Sheffield, Sheffield, S1 3JD, United Kingdom

(Received 30 December 1991)

The electroluminescence and current-voltage characteristics of a *p-i-n* double-barrier structure based on GaAs/AlAs are investigated. Electroluminescence lines due to carrier recombination in the GaAs contact layers and in the quantum well are observed. The bias dependence of the intensity of these lines exhibits the pronounced peaks that are also seen in the $I(V)$ characteristics, which are due to electron and hole resonant tunneling. The quantum-well emission lines correspond to recombination of holes in the two lowest-energy valence subbands (LH1 and HH1). Their relative intensities indicate that the hole population in these subbands is inverted over a wide range of bias. A rapid cooling of the holes is observed when the electron density in the quantum well is high.

Energy relaxation and recombination of electrons and holes in single- and multiple-quantum well systems and in superlattices and resonant tunneling devices have been extensively studied by means of optical techniques.[1-9] These have included time-resolved measurement and resonant tuning of quantum well (QW) levels with an external bias. Due to the speed of the intersubband and intrasubband relaxation processes, the steady-state populations of electrons in the higher-energy subbands of the QW are much lower than that in the ground state.[8-10] Nevertheless, in *n*-type superlattice structures, sufficiently high excited state populations have been achieved to produce radiative infrared emission due to electronic intersubband transitions.[10] Hot holes have also been observed in the first excited state of the valence-band quantum well.[5]

In this paper, we use a *p-i-n* double-barrier structure to resonantly inject holes into the excited states of the valence-band QW from the *p*-type side. Electroluminescence (EL) from the QW arises from recombination with confined electrons which are injected from the *n*-type side. We observe strong EL signals due to hole recombination in both the ground state and first excited states of the valence-band QW. We find that the hole population in these two states is inverted over a wide range of bias. At the bias voltages corresponding to electron resonant tunneling into the conduction-band QW, a large density of electrons builds up in the QW. A strong cooling effect of the holes in a normal thermal population in the QW is then observed. We attribute this to an Auger-like electron-hole interaction.

The composition of the device used in this investigation is shown in the inset in Fig. 1. The layer was grown by molecular-beam epitaxy on a (100) substrate and was processed into 100-μm-diam mesas with a 20-μm-thick outer annular metallic top contact. This allows efficient collection of the EL. The heavily doped n^+(Al,Ga)As top layer has a sufficiently wide band gap to transmit the EL from the 6.6-nm QW. Similar devices with QW widths of 5 and 8.2 nm were also investigated.

Figure 1 shows a band diagram of the device at a forward bias of around 1.65 V. Electron and hole accumulation layers form in the lightly doped spacer layers on the *n*-type and *p*-type sides of the two barriers. The excess negative (positive) charge in the electron (hole) accumulation layer is in the form of a quasi-two-dimensional electron (hole) gas with bound-state energy E_{ae} (E_{ah}) as shown in the figure. As the voltage is increased, both electrons and holes can resonantly tunnel from their respec-

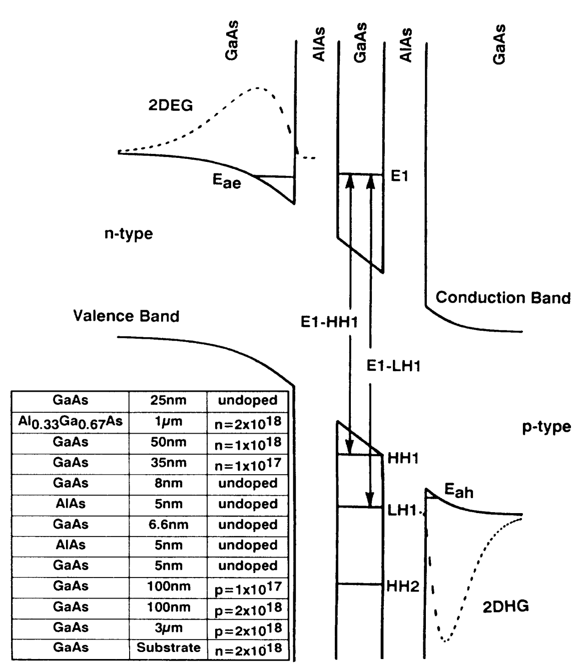

GaAs	25nm	undoped
$Al_{0.33}Ga_{0.67}As$	1μm	$n=2x10^{18}$
GaAs	50nm	$n=1x10^{18}$
GaAs	35nm	$n=1x10^{17}$
GaAs	8nm	undoped
AlAs	5nm	undoped
GaAs	6.6nm	undoped
AlAs	5nm	undoped
GaAs	5nm	undoped
GaAs	100nm	$p=1x10^{17}$
GaAs	100nm	$p=2x10^{18}$
GaAs	3μm	$p=2x10^{18}$
GaAs	Substrate	$n=2x10^{18}$

FIG. 1. A schematic diagram of the conduction- and valence-band profiles in the *p-i-n* double-barrier device at a forward bias of about 1.65 V. The inset shows the layer structure of the device; the doping densities are quoted in cm^{-3}.

tive accumulation layers into the quasi-bound states of the conduction- and valence-band QW's. The notation $E1$ refers to the conduction-band QW; HH1, LH1, HH2 refer to the heavy (HH) and light (LH) -hole states in the valence-band QW; the quantum number $(n=1,2)$ refers to the envelope function. This assignment is strictly applicable only for in-plane momentum, $k_{\parallel}=0$ when there is no light–heavy-hole admixing.

The forward bias current-voltage characteristic, $I(V)$, measured at 4.2 K, is shown in Fig. 2(a). Three strong resonant peaks are seen at 1.66, 1.707, and 1.797 V. An additional weak resonance at 1.59 V is observed in the conductance, dI/dV. A model which takes into account the quantum confinement energy of the conduction- and valence-band states in the QW and in the two accumulation layers gives the following ordering of these resonant features in $I(V)$ with increasing voltage: HH1, LH1, $E1$, HH2. This assignment is confirmed in separate measurements of $I(V)$ at high magnetic field.[11]

The EL occurs in two distinct spectral regions as shown in the plots in Figs. 3 and 4, taken at 4.2 K and various biases. The first at a photon energy of around 1.6 eV arises from recombination of electrons and holes in the QW; the second at around 1.5 eV from recombination in the bulk GaAs doping layers. The QW signal corresponds to two distinct lines: a *hot line* due to recombination of electrons in the $E1$ QW state with holes in the LH1 state and a *cold line* corresponding to $E1 \rightarrow$ HH1 transitions. Their energy separation (21 meV) corresponds to the LH1-HH1 splitting expected for a 6.6-nm QW. The EL signal due to bulk GaAs also consists of two distinct emission features at photon energies of 1.49–1.50 eV and of 1.518 eV. Their intensities are also strongly bias dependent. The lower-energy feature corresponds to electron recombination at neutral acceptors (e-A^0), while the higher energy feature is due to recombination of more weakly bound carriers (e-h, excitons or free hole recombination with electrons bound to shallow donors). The photon energies of all four lines have a weak dependence on voltage, though the $E1$-LH1 line shows a small redshift due to the quantum confined Stark effect[12] for above 1.8 V.

Although complete spectra were taken at a large number of fixed voltages (e.g., Figs. 3 and 4), a good indication of the intensity variation of the four lines can be obtained by setting the spectrometer at the peak of each line and sweeping voltage. The resulting curves are compared with the $I(V)$ characteristics in Fig. 2(b). The e-A^0 signal (spectrometer set at 1.490 eV) exhibits a sharp peak at 1.71 V, corresponding to the $E1$ resonance in $I(V)$ and two smaller peaks at 1.66 and 1.80 V, due to the LH1 and HH2 resonances. In contrast, the e-h signal (1.518 eV) shows the two hole resonances, with only a very weak feature corresponding to the strong $E1$ resonance in $I(V)$. Both e-A^0 and e-h curves show weak shoulders at around the HH1 resonance in dI/dV. We interpret their voltage dependence as follows. The absence of a strong $E1$ resonance in the intensity of the e-h line and the strength of this feature in the e-A^0 spectrum indicates that those resonantly tunneling electrons which do not recombine in the QW undergo recombination with termalized holes which

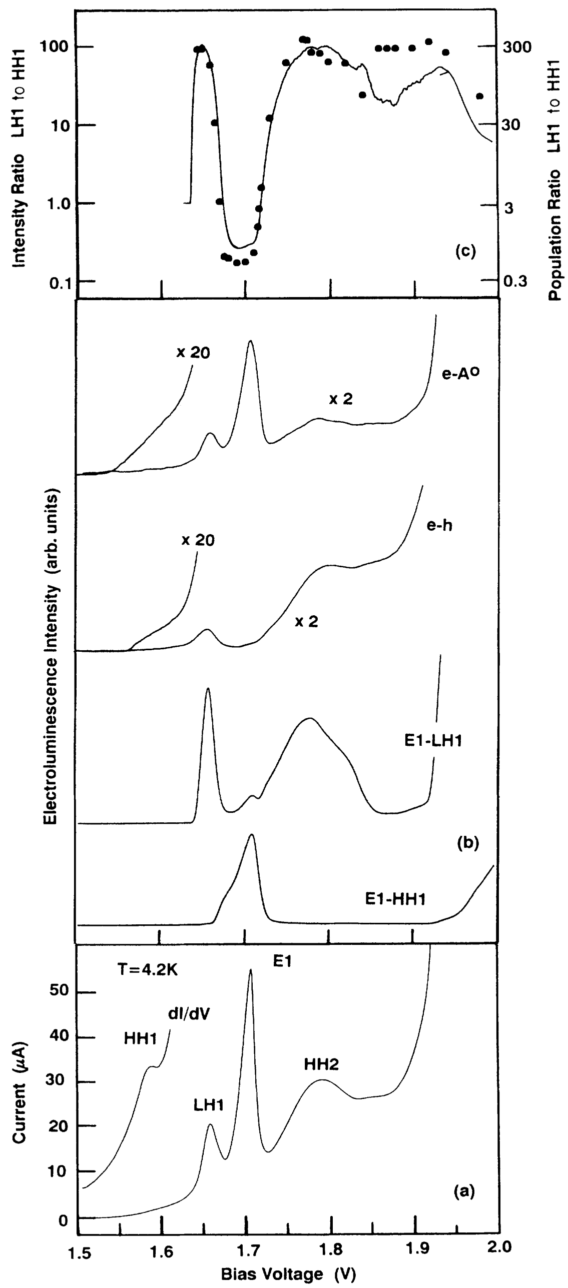

FIG. 2. (a) The current-voltage characteristics of the device measured at 4.2 K. The HH1 resonance is observed as a weak feature in the conductance, dI/dV. (b) The variation with bias of the electroluminescence intensity of the four emission lines observed. The spectra were taken with the spectrometer set at the peak of the emission lines, as described in the text with the device at 4.2 K. The intensities of the e-A^0 and e-h lines corresponding to recombination in the GaAs contact layers are weaker than the two QW lines ($E1$-HH1 and $E1$-LH1). For this reason, these plots are shown at higher gains (×2, ×20). (c) The variation with bias of the intensity ratio of the two electroluminescence lines associated with the QW. The continuous curve is obtained by taking the ratio of the $E1$-LH1 intensity shown in (b). The solid circles are obtained directly from the EL spectra at various biases. The population ratio shown on the vertical right-hand axis is obtained from the intensity ratio and from the relative oscillator strengths of the two transitions.

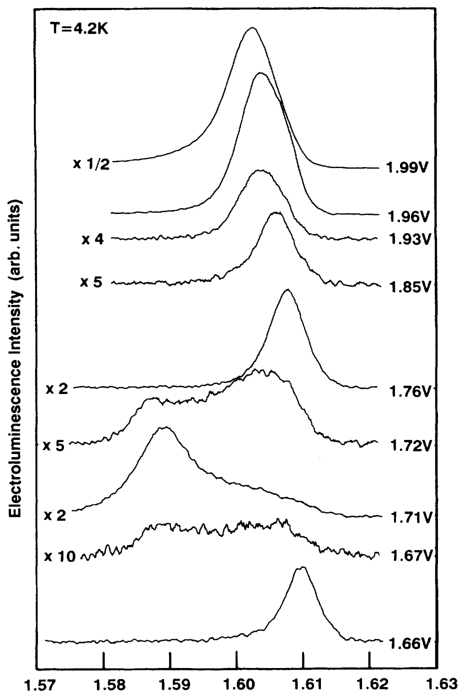

FIG. 3. Spectra (4.2 K) at various forward bias voltages of the electroluminescence arising from electron-hole recombination in the QW.

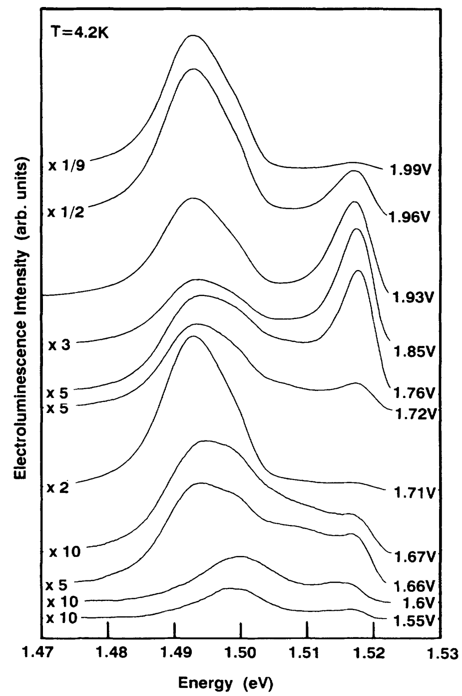

FIG. 4. Spectra (4.2 K) at various forward bias voltage of the electroluminescence arising from carrier recombination in the GaAs contact regions of the device.

are bound to neutral acceptors in the p-doped contact regions. The holes which pass through the QW in the regions of the LH1 and HH2 resonances either recombine as essentially free particles (e-h) in the n-type region or else bind to the residual acceptor impurities (e-A^0) prior to recombination. The e-A^0 recombination is relatively weaker for holes tunneling through the HH2 resonance than for the LH1 and HH1 features. This indicates that on the higher voltage HH2 resonance many of the hot holes injected into the n^- region are unable to relax all of their energy by shallow acceptor capture prior to recombination.

From Fig. 2(b), we see that the hot QW line (1.610 eV) dominates at voltages corresponding to the LH1 and HH2 resonances of the $I(V)$ curve. The cold QW line (1.589 eV) is only observed in the voltage range around the $E1$ resonance, where a large electron density is expected in the QW. From the intensity ratio of the two QW lines and their relative oscillator strengths (1:3, see Ref. 13), we determine the population ratio of holes in the LH1 and HH1 states of the QW, as shown in Fig. 2(c). The continuous curve is obtained from the ratio of the LH1 and HH1 EL intensity plots in Fig. 2(b); the solid circles are obtained directly from analysis of the EL spectra at fixed voltages. Above 1.9 V, when the Stark shift of the hot line becomes significant, the continuous curve is unreliable. The hole populations in the HH1 and LH1 states of the valence-band QW's are strongly inverted, except for the voltage range corresponding to the $E1$ resonance. The background noise level permits us to measure the LH1 to HH1 intensity ratio up to a value of approximately 100:1. Therefore we can estimate that the population ratio is $\gtrsim 300$ at the peaks of the LH1 and HH2 resonances.

The existence of EL from the QW over the entire range of bias above 1.67 V indicates the presence of both electrons and holes in the QW, even when the device is biased at off-resonance points. In the region of the LH1 and HH2 resonances and above 1.8 V, where the hole population inversion is most pronounced, the electron density in the QW is relatively small ($< 10^{10}$ cm^{-2}). This is because the device is biased well away from $E1$ resonance and electrons can only enter the QW due to nonresonant

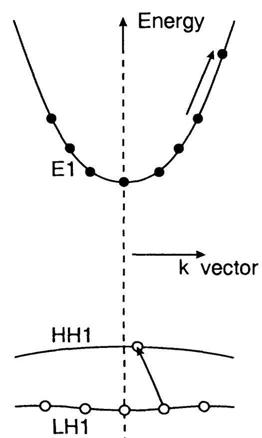

FIG. 5. A schematic diagram showning the Auger-like process in which hot holes in the LH1 subband of the valence-band QW lose energy to electrons in the $E1$ subband of the conduction-band QW.

processes. In all three devices in which we have observed a population inversion, the energy separation of the HH1 and LH1 states is less than that of the longitudinal optic (LO) phonon ($\hbar\omega_L = 36$ meV for GaAs). Hence holes which enter the LH1 state, either directly on the LH1 resonance or else indirectly on the HH2 resonance by intersubband scattering (HH2→LH1), are unable to emit LO phonons. The LO-phonon emission rate of holes is fast ($\sim 10^{13}$ s^{-1}),[14,15] but only when energetically possible, i.e., in sufficiently narrow QW's. Our results indicate that the transition rate ($\tau_{2,1}^{-1}$) from LH1 to HH1, either by acoustic-phonon emission or infrared emission (forbidden at zero bias) is much slower[16] than the rate of loss of holes from the HH1 state by tunneling (τ_{1t}^{-1}) or electron-hole recombination (τ_{1r}^{-1})$\sim 10^9$ s^{-1}.[17,18] The LH1 state is thus a bottleneck for cooling of holes. On the $E1$ resonance, the electron density in the QW is high ($\sim 10^{11}$ cm^{-2}).[11] We attribute the observed cooling of the hole population in the voltage region of this resonance to Auger processes[19] in which a hole relaxes from LH1 to HH1, transferring its energy and momentum to an electron in E1 (see Fig. 5). It is surprising that the hole population inversion is so marked on the HH2 resonance since the HH2→HH1 transition is energetically possible via LO emission. Further calculations of this and other transition rates would be of value.

In summary, we have used a *p-i-n* double-barrier structure to resonantly inject electrons and holes into a quantum well. Population inversion of holes in the HH1 and LH1 subbands is observed over a wide range of bias but is quenched by an Auger process when electron density in the well is high ($\sim 10^{11}$ cm^{-2}).

This work is supported by the Science and Engineering Research Council (United Kingdom).

[1]A. Pinczuk, J. Shah, R. C. Miller, A. C. Gossard, and W. Wiegmann, Solid State Commun. **50**, 735 (1984).

[2]J. Shah, Solid-State Electron. **32**, 1051 (1989), and references therein.

[3]J. F. Ryan, Physica B **134**, 403 (1985).

[4]W. W. Rühle, M. G. W. Alexander, and M. Nido, in *Proceedings of the Twentieth International Conference on the Physics of Semiconductors, Thessaloniki, Greece, 1990,* edited by E. M. Anastassakis and J. D. Joannopoulos (World Scientific, Singapore, 1990), p. 1226.

[5]H.-J. Polland, W. W. Rühle, J. Kuhl, K. Ploog, K. Fujiwara, and T. Nakayama, Phys. Rev. B **35** 8273 (1987).

[6]D. Bimberg, J. Christen, A. Steckenborn, G. Weimann, and W. Schlapp, J. Lumin. **30**, 562 (1985).

[7]J. F. Young, B. M. Wood, H. C. Liu, M. Buchanan, D. Landheer, A. J. Springthorpe, and P. Mandeville, Appl. Phys. Lett. **52**, 1398 (1988).

[8]M. S. Skolnick, D. G. Hayes, P. E. Simmonds, A. W. Higgs, G. W. Smith, H. J. Hutchinson, C. R. Whitehouse, L. Eaves, M. Henini, O. H. Hughes, M. L. Leadbeater, and D. P. Halliday, Phys. Rev. B **41**, 10754 (1990).

[9]H. T. Grahn, H. Schneider, W. W. Rühle, K. von Klitzing, and K. Ploog, Phys. Rev. Lett. **64**, 2426 (1990).

[10]M. Helm, P. England, E. Colas, F. DeRosa, and S. J. Allen, Jr., Phys. Rev. Lett. **63**, 74 (1989).

[11]P. M. Martin, R. K. Hayden, C. R. H. White, M. Henini, L. Eaves, D. K. Maude, J. C. Portal, G. Hill, and M. A. Pate, in *Proceedings of the International Conference on Hot Carriers in Semiconductors, 1991* [Semicond. Sci. Technol. **7**, 456 (1992), special issue].

[12]D. A. B. Miller, D. S. Chemla, T. C. Damen, A. C. Gossard, W. Wiegmann, T. H. Wood, and C. A. Burrus, Phys. Rev. B **32**, 1043 (1985).

[13]G. Bastard, *Wave Mechanics Applied to Semiconductor Heterostructures* (Les Éditions de Physique, Paris, 1988).

[14]D. von der Linde and R. Lambrich, Phys. Rev. Lett. **49**, 1090 (1979).

[15]R. W. Kelsall, A. C. G. Wood, and R. A. Abram, Semicond. Sci. Technol. **6**, 841 (1991).

[16]The steady-state population ratio of LH1 and HH1 is $\sim \tau_i(\tau_{1r}^{-1} + \tau_{1t}^{-1})$.

[17]T. Matsusue and H. Sakaki, Appl. Phys. Lett. **50**, 1429 (1987).

[18]H. W. Liu, C. Delalande, G. Bastard, M. Voos, G. Peter, R. Fischer, E. O. Göbel, J. A. Brum, G. Weimann, and W. Schlapp, Phys. Rev. B **39**, 13537 (1989).

[19]R. I. Taylor, R. Abram, M. G. Burt, and C. Smith, IEE Proc. Part J: Optoelectron. **132**, 364 (1986).